ELSEVIER

Recent advances and remaining challenges in thin-film silicon photovoltaic technology

F. Meillaud*, M. Boccard, G. Bugnon, M. Despeisse, S. Hänni, F.-J. Haug, J. Persoz, J.-W. Schüttauf, M. Stuckelberger and C. Ballif

Ecole Polytechnique Fédérale de Lausanne (EPFL), Photovoltaics and Thin-Film Electronics Laboratory, Rue de la Maladière 71b, CH-2000 Neuchâtel, Switzerland

This contribution reviews some of the latest achievements and challenges in thin-film silicon photovoltaic (PV) technology based on amorphous and nanocrystalline silicon and their alloys. We address material and device developments, including (i) improved plasma deposition processes to achieve high-quality dense absorber materials; (ii) absorber layers based on silicon tetrafluoride, which lead to enhanced absorption in the near-infrared and yield outstanding short-circuit current densities; (iii) dedicated optimization of the interfaces and device architecture, as well as (iv) enhanced light harvesting by means of multi-scale textured substrates and reduced parasitic absorption in the non-active layers. This paper will describe how, by combining all of these advances along with precise control of plasmas over large areas, key results have been achieved in recent years, at both the cell and large-area module level, with stabilized efficiencies of over 13 and 12%, respectively.

Introduction

Thanks to a continuous and remarkable growth rate over the last 10 years, photovoltaics (PV) have now exceeded 100 gW-peak of worldwide cumulative installed capacity [1]. PV is thus well on its way to becoming a conventional source of electricity, with today's very low module prices making it appealing to investors and private individuals. Crystalline silicon (c-Si) dominates the market, with thin-film technologies based on cadmium-telluride (CdTe), copper–indium–gallium–selenide (CIGS) and silicon taking around 10% of the market. Thin-film silicon technology presents numerous advantages, including: (i) the raw materials are abundant and non-toxic [2], (ii) rigid or flexible – and possibly lightweight – substrates can be used [3], (iii) its uniform appearance is well suited for building integration [4,5]. Thin-film silicon modules can also be easily patterned by laser, allowing various degrees of transparency. The major drawback of thin-film silicon technology is its lower conversion efficiency, which is in the range of 7–10% for commercial modules versus 15–21% for those based on c-Si.

Thin-film silicon devices are based on either amorphous silicon (a-Si:H) or microcrystalline (also called nanocrystalline) silicon (μc-Si:H). Because of its amorphous network, a-Si:H is more defective than c-Si and suffers from a performance degradation upon light soaking, known as the Staebler–Wronski effect (SWE) [6]. This degradation phenomenon is much less severe in μc-Si:H, which is a mixed-phase material composed of interconnected nanocrystalline grains (usually less than 30 nm in size) embedded in an amorphous matrix. During μc-Si:H layer growth, large conglomerates of nanocrystals form, with typical sizes on the order of hundreds of nanometers. This complicated, still fascinating, material is not yet fully understood. Its microstructural and electronic properties depend in a complex manner on the deposition parameters and on the structure of the substrate. This explains why a major part of the research efforts during the last 10 years has focused on further understanding thin-film silicon material properties and growth. Emphasis was also placed on developing thinner devices, which reduces not only deposition time and thus production costs, but also light-induced degradation (LID) in a-Si:H, since the thicker the absorber layer, the larger the impact of the SWE on solar cell performance. It must also be mentioned that doped layers have poor electronic properties. Hence only intrinsic,

*Corresponding author:. Meillaud, F. (fanny.sculati-meillaud@epfl.ch)

 http://dx.doi.org/10.1016/j.mattod.2015.03.002

that is undoped, material can be used as the absorber, with still a modest minority-carrier lifetime. Consequently, the use of p-i-n junctions with an electric field extending throughout the device is required, and not p-n junctions like most other PV technologies [7].

Thin-film silicon solar cells and modules can be made in two different configurations: the superstrate configuration, also called 'p-i-n' in accordance with the sequence of layers, or the substrate ('n-i-p') configuration. In superstrate configuration, light enters through the substrate, typically glass, while in the substrate configuration, light enters through the last layer to be deposited (light always enters through the p-type layer, because of the poorer mobility of holes). Whereas glass is most widely used in the superstrate configuration, a large variety of substrates have been employed for the substrate configuration, including stainless steel and flexible foils such as polyethylene naphthalate (PEN) or polyimide. This latter polymer was, for example used by United Solar Ovonic Corporation, one of the pioneers in the development of flexible thin-film silicon modules, fabricated by roll-to-roll processing [7–9]. Flexible modules present distinctive advantages for building integration (BIPV) with their light weight, a certain freedom in design for, for example curved building parts, and reduced mounting costs. Indeed, these products can be directly bonded to the roof or directly laminated with building elements [10]. However, the BIPV market has not yet developed as expected and many manufacturers of flexible thin-film silicon solar cells had to stop their production.

The goal of this contribution is to describe the latest advances in thin-film silicon PV research, with, first, a review on state-of-the art efficiencies of solar cells and modules. Then, the paper will depict how a high-quality dense absorber material, together with a dedicated optimization of the interfaces and device architecture, is mandatory to reach high conversion efficiencies. Furthermore, routes on how to increase the short-circuit current density in such thin solar cells will be discussed in view of: (1) the use of silicon tetrafluoride (SiF_4), leading to enhanced absorption in the near-infrared, as well as (2) the development of multi-scale textured substrates and more transparent non-active layers.

State-of-the-art efficiencies

Nowadays, mainstream thin-film silicon research deals with multi-junction solar cells, as obtained by the monolithic interconnection of at least two sub-cells. The 'micromorph tandem' [11] is, for example obtained by combining an a-Si:H top cell with a μc-Si:H bottom cell, as sketched in Fig. 1 in the superstrate configuration. Transparent conductive oxide (TCO) materials – typically tin oxide (SnO_2), zinc oxide (ZnO) or indium tin oxide (ITO) – are used as front electrodes. A metallic electrode or a TCO material and a dielectric white reflector are used in the back. An intermediate reflecting layer (IRL) is typically implemented between the top and bottom cells as sketched in Fig. 1. This layer, generally based on silicon oxide (SiO_x) material, reflects light into the top cell, thanks to its lower refractive index (typically $n \sim 1.7$–2 at 600 nm) compared to that of silicon ($n_{Si} = 3.8$), allowing for a thinner top cell. However the IRL needs to be conductive enough and as transparent as possible to reduce absorption losses. As will also be discussed later in this contribution, certain SiO_x layers fulfill these conditions and furthermore can be mixed-phased, with the alloying

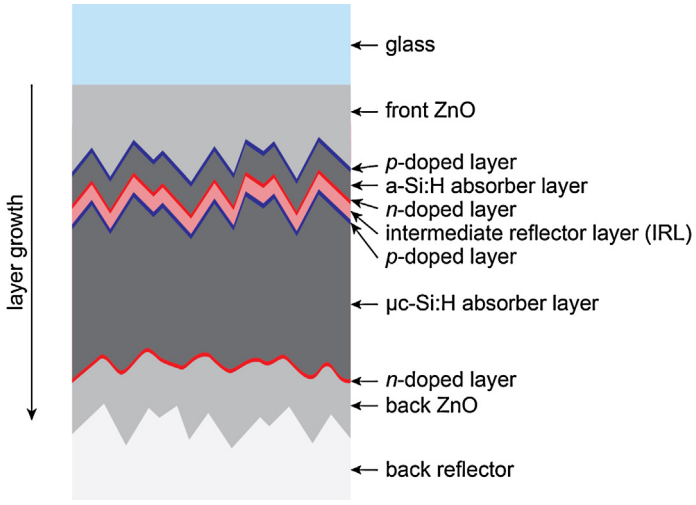

FIGURE 1

Schematic of a typical amorphous (a-Si:H)/microcrystalline silicon (μc-Si:H) (micromorph) tandem in the superstrate configuration. Light enters through the glass and front electrode, here composed of zinc oxide (ZnO). The a-Si:H cell is the top cell, whereas the bottom cell is composed of μc-Si:H. An intermediate reflecting layer (IRL) is typically implemented between two cells to increase the current density of the top cell. ZnO is then used as the back electrode in combination with a reflector.

taking place in the amorphous phase of the layer, while silicon crystallites evolve as filaments [12]. Much work has been undertaken on the topic of IRLs (see, e.g. [13–15]), with the latest developments focusing on asymmetric morphologies in both the superstrate [16,17] and substrate [18] configurations, to optimize both light trapping and absorber layer growth.

Thin-film silicon is particularly suitable for multi-junctions as it offers a wide range of bandgaps (see, e.g. [19] for a-Si:H). Multi-junctions, also widely used in other PV technologies such as those based on III-V compounds (see, e.g. [20]), enhance efficiency by either extending or more efficiently using the absorbed light spectrum [21,22]. For thin-film silicon, the use of the multi-junction configuration also generally leads to reduced LID of the solar cell performance, thanks to the use of thinner a-Si:H absorber layers. Furthermore, the multi-junction configuration not only increases open-circuit voltage (V_{oc}) values through the monolithic interconnection, it also reduces resistive losses in the electrodes – and therefore increases the fill factor (FF) – because of the lower short-circuit current density (J_{sc}). Multi-junctions thus allow for the use of more resistive, and hence more transparent, electrodes.

The intense research efforts of the last years have recently led to novel record certified stabilized device efficiencies for both single-junction [23–25] and multi-junction solar cells [26], as reported in Table 1. The highest stabilized certified efficiency now stands at 13.4% for a small-area cell in the triple-junction configuration [27], while the best micromorph tandem modules now reach over 12% stabilized efficiency [28], an impressive result on 1.4 m^2. Furthermore, it was already demonstrated that conversion efficiencies of over 10% could be maintained, in superstrate configuration, over areas as large as 5.7 m^2 [29]. Table 1 hence demonstrates that the continuous progress achieved over the last years has permitted to reduce the gap between the efficiencies of solar cells (~1 cm^2) and modules (>1 m^2). Still, commercial

TABLE 1

Best certified stabilized efficiencies for thin-film-silicon–based devices (cells and modules) of up to three junctions.

Device type	Area (cm^2)	Certified stabilized efficiency (%)	Laboratory
a-Si:H	1.036	10.1	Oerlikon Solar Lab [23]
a-Si:H	1.001	10.2	AIST [25]
μc-Si:H	1.045/1.045	11.0/11.4	AIST [24]/AIST [31]
a-Si:H/μc-Si:H	1.001	12.6	PV-Lab, EPFL [26]
a-Si:H/μc-Si:H	14322	12.2	TEL Solar AG [28]
a-Si:H/μc-Si:H/μc-Si:H	1.006	13.4	LG Electronics [27]
a-Si:H/a-SiGe:H/μc-Si:H	399.8	12.0	United Solar [32]
a-Si:H/a-SiGe:H/μc-Si:H	14305	10.9	LG Electronics [33]

thin-film silicon modules are rather in the range of 9.6–10.4% for modules on glass with manufacturers including NexPower, Kaneka, Sharp, Hanergy, Sun Well, and 3sun, and 7% (a-Si:H) to 10% (tandem a-Si:H/μc-Si:H) for flexible modules with, for example HyET Solar and F-Wave. Since the market is now particularly competitive with low-priced c-Si modules, thin-film silicon modules face strong pressure to enhance efficiency, even with announced production costs as low as 0.35–0.40 €/W_p (Oerlikon Solar). Indeed, for traditional PV systems (rooftop or commercial), the so-called area-related balance-of-system costs (see, e.g. [30]) put low-efficiency modules at a competitive disadvantage.

To further increase the efficiency, the potential of innovative absorber materials combined with dedicated device structures must now be confirmed at the research level. We expect that, by combining all recent advances, stabilized efficiencies on the order of 14% (with, e.g. V_{oc} = 1.42 V, FF = 71%, and J_{sc} = 14 mA/cm^2) are within reach for tandem devices, instead of the present ~12.6% achieved on a small scale (~1 cm^2) [26]. Furthermore, an additional efficiency potential of 1–2% absolute can be expected for devices with up to four junctions. Indeed, while an impressive 16.3% initial efficiency was already demonstrated by United Solar in triple-junctions configuration [34], with a middle cell composed of amorphous silicon alloyed with germanium (a-Si:H/a-SiGe:H/μc-Si:H), a maximum initial conversion efficiency of 19.8% has been theoretically projected with quadruple-junctions [35].

Finally, we should also mention the recent rapid developments of crystalline silicon thin-film (c-SiTF) solar cells obtained by liquid-phase crystallization (LPC) of amorphous or microcrystalline films some tens of micrometers thick [36,37]. With this technique, solar cells with initial efficiencies up to 11.8% have been achieved with a high V_{oc} value of 632 mV [38].

Absorber material: dense and of high-quality

The most common fabrication method for thin-film silicon is plasma-enhanced chemical vapor deposition (PECVD), typically achieved from silane (SiH_4) and hydrogen (H_2) in capacitively coupled reactors. The plasma is excited with an AC signal, at a frequency of 13.56 MHz (radio frequency – RF) or above (very high frequency – VHF) (see, e.g. [39,40] for details on the effects of frequency on plasma). Other hardware characteristics affecting the plasma include the inter-electrode distance [41,42] and the electrode geometry [43,44]. The structure of thin-film silicon material can be modified, possibly in the same reactor, from fully a-Si:H to highly μc-Si:H simply by adjusting the deposition conditions (SiH_4/H_2 ratio, power, pressure, temperature) [45,46]. As previously mentioned, μc-Si:H is a mixed-phase material composed of nanocrystalline grains evolving into conglomerates on the order of a few hundreds of nanometers. However, nanoporous regions may also appear during the layer growth, particularly in μc-Si:H but also in a-Si:H [47], typically because of an inappropriate (front electrode) starting morphology, as will be discussed later. The crystalline fraction of μc-Si:H layers is generally assessed by Raman spectroscopy [48], with an optimum Raman crystallinity factor (R_c) value of ~ 60% for the absorber layer [45,49], while the use of SiF_4 during PECVD yields R_c values of up to 90% [50].

The microstructural change that occurs during the transition from a-Si:H to μc-Si:H also impacts the bandgap value which is reduced from 1.75 to 1.1 eV, while alloying, for example with germanium, further modifies the bandgap. Even though the lower bandgap of μc-Si:H enables better absorption of the near-infrared spectrum, its indirect bandgap leads to reduced light absorption, and absorber thicknesses in the range of 1–3 μm are necessary to achieve a sufficient J_{sc}. A weakness of μc-Si:H lies in its low deposition rate for high-quality material, typically below 0.5 nm/s. Efforts have thus been made to increase the deposition rate, as by, for example employing a larger plasma power density [51] or a higher excitation frequency such as VHF [52]. At RF, the well-known 'HPD' (high-pressure depletion) regime [53,54] has led to μc-Si:H solar cells with efficiencies of over 8.5% with the absorber layer grown at rates of more than 3 nm/s [55,56]. Furthermore, a micromorph module with a stabilized conversion efficiency of 10% was deposited at 2.4 nm/s on 1.43 m^2 using localized plasma confinement [57].

A characteristic of μc-Si:H is its sensitivity to growth conditions and, more precisely, its dependence on substrate surface chemistry and morphology [58–60]. It has been known for years that defective (nanoporous) zones may appear in silicon [61–63] when it is deposited on an inappropriate surface texture, resulting in the formation of a 2-D network [64]. Even though ZnO grown by low-pressure chemical vapor deposition (LPCVD) is considered to be one of the best electrode materials for thin-film silicon solar cells on glass, it may present an inadequate surface for high-quality silicon growth because of its roughness and V-shaped morphology [65]. For this reason, in 2006, a plasma-based surface treatment of as-grown LPCVD ZnO was proposed to smoothen the V-shaped valleys [66], at the cost of a reduced J_{sc} due to poorer light trapping. PECVD process conditions and substrate temperature can also strongly influence the formation of these nanoporous regions and reduce their density [67,68]. An example of the influence of both substrate morphology and process conditions on μc-Si:H growth is shown in Fig. 2.

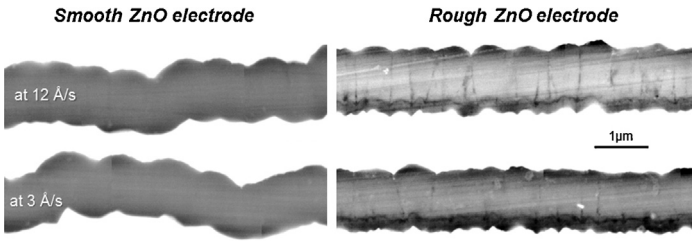

FIGURE 2

Scanning electron microscopy (SEM) images of µc-Si:H layers deposited on smooth and rough front electrodes, with growth rates of 3 and 12 Å/s. On the smooth electrode, no porous zone can be highlighted, even for the growth rate of 12 Å/s (the layer material is homogenous). On the rough electrode, nanoporous zones clearly appear as dark vertical lines. Nanoporous zones can either form at the beginning of the µc-Si:H layer or later during the growth. The density of nanoporous zones is larger at higher growth rate on the rough electrode.

Very recent work [69] suggests that the two most common excitation frequencies used in PECVD reactors, that is RF and VHF, can both lead to the growth of a very good bulk material quality, as derived from Fourier transform photocurrent spectroscopy (FTPS) measurements. However, on rough substrates and at a low growth rate, RF leads to denser µc-Si:H material and, hence, better solar cell performance. A general trend for conversion efficiency as a function of growth rate is sketched in Fig. 3 for solar cells deposited on rough substrates with RF or VHF. Based on the major growth models proposed for thin-film silicon [70], the layer densification could result from an increase in ion bombardment occurring at low frequency, while VHF leads to reduced sheath thickness and enhanced contribution of highly reactive radicals, such as silylenes (SiH_2), with the growth of a more porous silicon material. Still, the impressive result achieved by TEL Solar

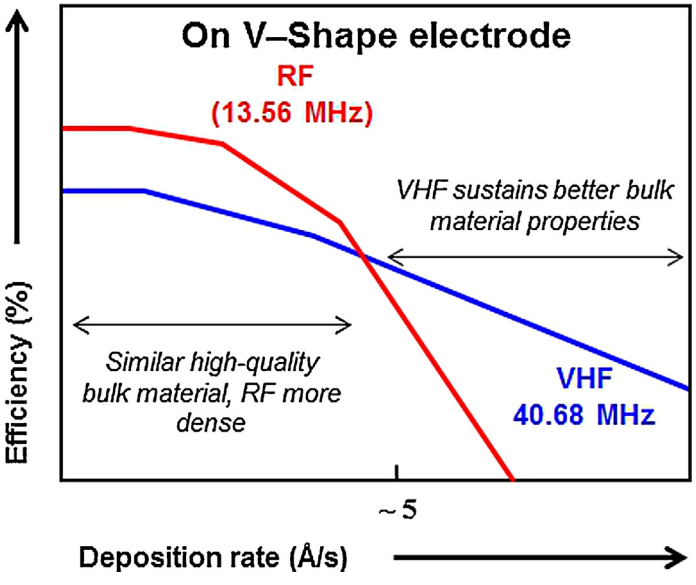

FIGURE 3

Schematic of the general trend for µc-Si:H single-junction solar cell conversion efficiency as a function of growth rate, at 13.56 MHz (RF) and 40.68 MHz (VHF), when deposited on a front electrode presenting a rough, V-shaped morphology, favorable to the creation of porous zones. For low growth rates, RF provides both a high-quality bulk and a dense material, while at higher growth rates VHF sustains a better bulk quality (see the detailed study in [69]).

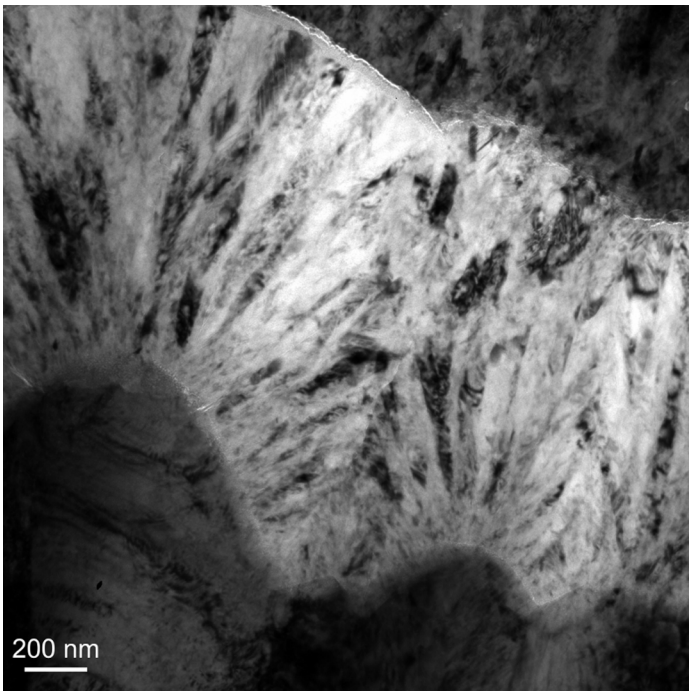

FIGURE 4

Bright-field transmission electron microscopy (TEM) cross-section of a µc-Si:F:H single-junction solar cell with large crystalline grains that are clearly visible (see [75] for more details).

with a stabilized module efficiency of 12.24% was obtained at VHF, with processes taking place at high pressure and with a very small inter-electrode distance [71]. Note that nanoporous zones impact not only the initial electrical performance of µc-Si:H-based solar cells but also their stability over time, because of post-oxidation mechanisms (see, e.g. [55,72]).

In order to overcome the trade-off between V_{oc} and J_{sc} as typically imposed by the interplay between substrate roughness and silicon growth quality, the use of fluorinated gas precursors, such as SiF_4, has been suggested. First reports on the use of fluorinated precursors for the fabrication of thin-film silicon layers date back to the 1970s (see, e.g. [73]). Kasouit et al. later demonstrated that the addition of small amounts of SiF_4, highly diluted in Ar, to H_2, result in highly crystallized thin-film silicon layers with R_c values of 90%, above those of standard µc-Si:H (generally limited to about 80–85%) [50]. It was then reported [74] that nanocrystals already form in the plasma and that the crystallization process is further supported by preferential etching of the amorphous phase. Transmission electron microscopy (TEM) measurements performed at PV-Lab on fluorinated microcrystalline silicon (µc-Si:F:H) solar cells confirm the growth of large columnar grains, see Fig. 4, for a R_c of 90%. Unfortunately, multiple growth defects were also seen, including stacking faults and nanoporous regions, leading to low V_{oc} values in single-junction solar cells [75]. Still, V_{oc} values above 500 mV were already demonstrated for highly crystallized absorber layers [76,77], leading to solar cells efficiencies of over 9% [77].

Furthermore, the exceptionally high crystallinity and large grain size of µc-Si:F:H layers lead to enhanced absorption in the near-infrared, as discussed in [78] and as shown in Fig. 5. This figure compares external quantum efficiency (EQE) curves for two micromorph cells of similar thicknesses with the bottom-cell

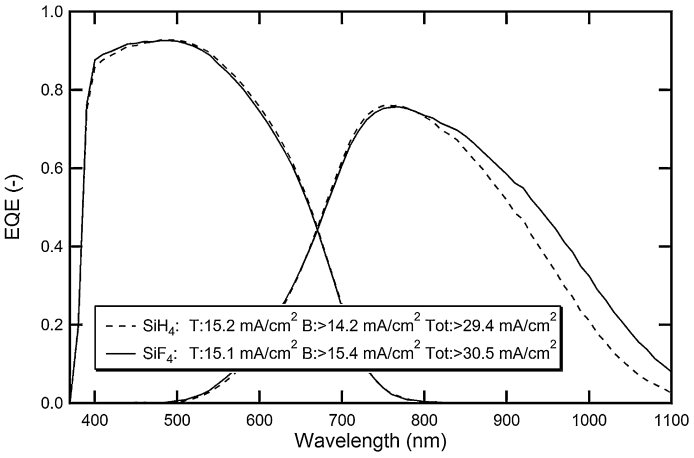

FIGURE 5

External quantum efficiency (EQE) curves, and corresponding top (T), bottom (B), and total (Tot) current densities of two tandem devices with a 250-nm-thick a-Si:H top cell, a 70-nm-thick IRL, and a 3.1-μm-thick, highly crystallized, bottom cell absorber layer deposited from SiH_4- or SiF_4-based plasmas. Increased absorption in the near-infrared can be observed for the μc-Si:F:H absorber layer, leading to a gain of 1.1 mA/cm^2. EQE were measured at 0 V with an antireflective foil applied on the glass.

absorber layer deposited from a SiH_4- or SiF_4-based plasma. A J_{sc} value above 15 mA/cm^2 is obtained in the top cell thanks to the use of a 70-nm-thick IRL, while a J_{sc} gain of 1.1 mA/cm^2 is achieved in the bottom cell, with the enhanced absorption in the near-infrared. In the best case, an outstanding total J_{sc} of 31.9 mA/cm^2 was reached in a tandem incorporating μc-Si:F:H for a total silicon thickness of less than 3.5 μm [75].

Finally, as thin-film silicon multi-junction solar cells use amorphous silicon as the top-cell absorber material, researchers have also investigated deposition conditions that lead to more stable a-Si:H material with respect to light soaking. Different materials and deposition conditions have been presented as best candidates for stable high-efficiency solar cells, including: (i) a-Si:H deposited at low pressure and VHF, with rather low hydrogen dilution, in a standard parallel-plate reactor [79] or with a mesh in the triode configuration [80], (ii) protocrystalline silicon (pc-Si:H) [81] and (iii) polymorphous silicon [82]. A systematic comparison of these various materials and deposition conditions can be found in [83]. A low-pressure, low-dilution a-Si:H process led, in 2009, to a certified stabilized efficiency of 10.1% [23], overtaken only this year by a certified 10.2% conversion efficiency achieved by AIST in a triode reactor, as just announced at the 29th EU PV conference [25]. The triode configuration leads to the lowest LID of 10% for a standard thickness of 250 nm as opposed to at least 15% for devices grown with standard PECVD [84]. Furthermore, Matsui et al. demonstrated that, with such a reactor configuration, the lower LID can be maintained for increased thicknesses of up to ~400 nm, which is not the case for standard a-Si:H.

Dedicated interfaces and device architecture

The multi-junction approach as path to higher conversion efficiency requires optimum light harvesting together with the growth of high-quality, dense, material. As this latter point has just been discussed in the previous paragraph, we shall now focus on recent advances toward better light management and dedicated device architecture. First, reflections are typically reduced by either applying a texture to glass or by adding an anti-reflecting layer of adequate refractive index, at the air-glass [85,86] or glass-ZnO [87] interface. Second, and as previously mentioned, the substrate and front electrode surface features are commonly chosen to offer the best compromise between efficient light trapping and high-quality silicon growth. In order to overcome this tradeoff, electrodes consisting of a combination of various textures have been developed, such as large-smooth and small-sharp, as reported by Asahi Glass Co in 2007 with SnO_2 [88]. In 2010, Oerlikon Solar combined textured glass and ZnO to achieve an 11.9% stabilized micromorph tandem efficiency, a record at that time [89]. The multi-scale concept was then further developed with nanoimprint and nanomoulding techniques [90,91] in which a desired texture is reproduced in a transparent resin, decoupling the optical and electrical features of the electrode, leading to an initial micromorph efficiency of 14.1% [92]. In the substrate configuration, novel types of morphologies were successfully implemented as well, such as the 'honeycomb' texture [93] and 'optically rough-physically flat' substrates described in [94,95]. Furthermore, a recent trend in PV is the development of nanowires and radial-junction solar cells with, for example the ~8% stabilized conversion efficiency achieved by S. Misra et al. [96] for an a-Si:H absorber layer only 100 nm thick.

However, good light trapping is not sufficient to get high J_{sc} values. Absorption in the non-active layers of the solar cells, that is the electrodes, the doped layers and the IRL, must also be reduced [97,98]. In the case of ZnO electrodes, parasitic absorption can be decreased by, for example reducing the free-carrier density in the layer [99,100] or by applying a post-deposition treatment [101,102]. One can also use high-mobility electrode materials such as hydrogenated indium oxide (In_2O_3:H) [103,104], while, at the back of the cell, use of photonic crystals has been evaluated [105,106]. Additionally, solutions for lowering parasitic absorption in doped layers have also been proposed, such as the use of SiO_x [107,108], as in IRLs, or silicon carbide (a-SiC:H) layers [109,110]. The mixed-phase microstructure of SiO_x material results not only in an increased bandgap, but also in reduced lateral conductivity as compared to standard μc-Si:H doped layers. This decrease in conductivity leads, in turn, to a greater resilience of thin-film silicon solar cells to substrate roughness, attributed to a shunt-quenching effect [111].

Finally, interfaces can also be improved by implementing a buffer layer, based, for example on SiO_x [112], SiC:H [113] or even intrinsic a-Si:H [114,115], between the doped layers and the absorber. With an intrinsic a-Si:H buffer layer, V_{oc} values exceeding 600 mV were reached in very thin μc-Si:H solar cells, where performances are limited by defects at the interfaces and not in the absorber material, demonstrating a clear passivation effect [116].

Conclusions and prospects

The last decade has seen a huge industrial effort to upscale thin-film silicon technologies. This upscaling can be considered successful, as the difference in conversion efficiency between cells and modules is the lowest of all PV technologies (see Table 1). In parallel, a huge step has been made in both thin-film silicon material and device understanding with the identification of the possible interlinks between the substrate morphology and the plasma process

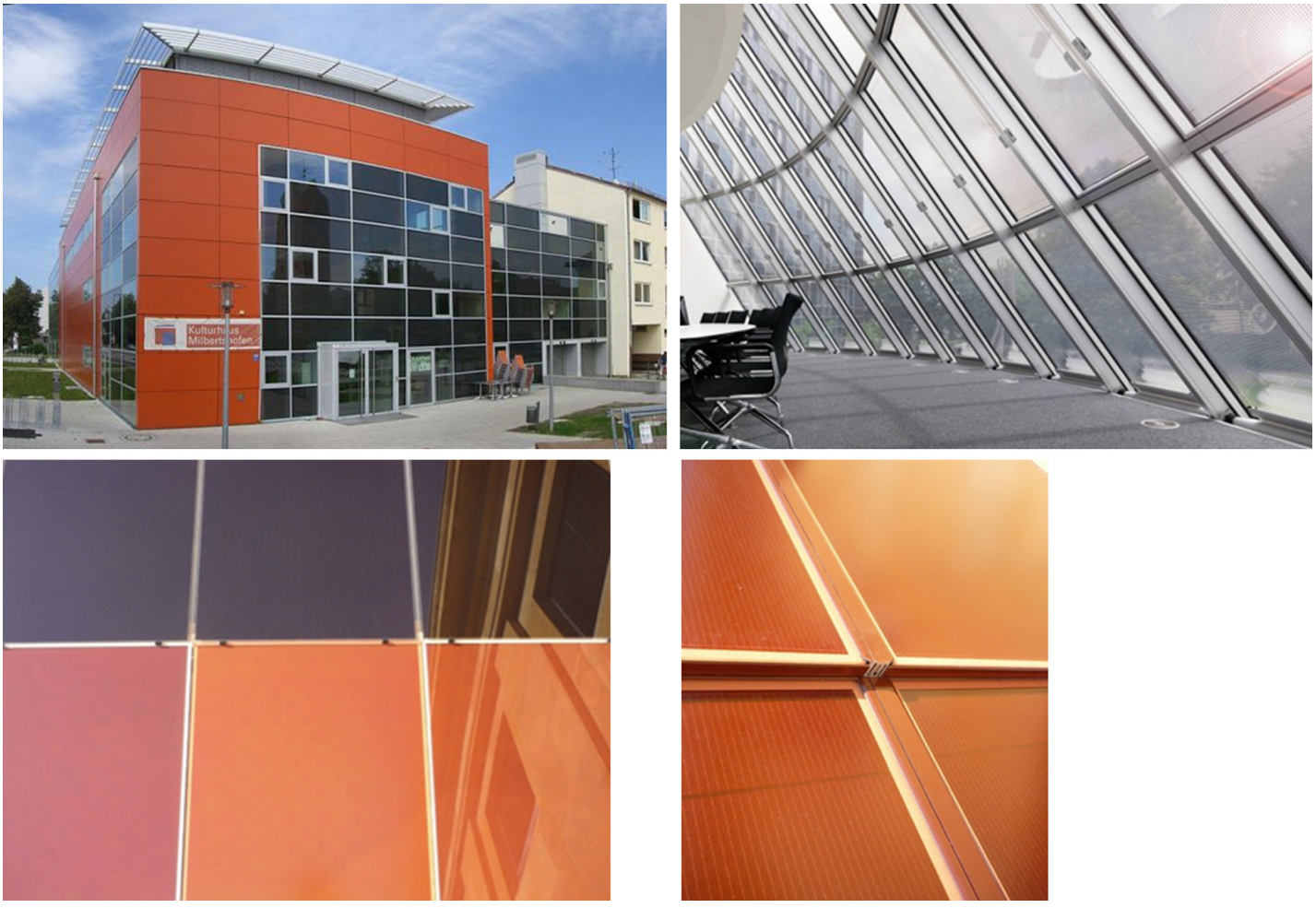

FIGURE 6

Example of thin-film silicon integration into buildings: top left) Kulturhaus Milbertshofen (Germany); top right) Semi-transparent, large-area, custom-size semi-transparent a-Si:H modules (Malibu GmbH); bottom left) Variation of colors of thin-film silicon modules; bottom right) Detailed view of a 'terracotta' thin-film silicon module (see also [5] for additional examples).

conditions, and the device architecture and parasitic losses in solar cells. Enhanced light harvesting was demonstrated via dedicated decoupling of the optical and electrical characteristics of the substrate from the front electrode, thanks to, for example nanoimprint and nanomoulding technologies.

Considering the key results achieved the last years, at both the lab and production scale, the potential for solar cells with 15% or even 16% stabilized efficiency can be foreseen. Further efficiency improvements would necessitate breakthrough advances in the absorber material, with further research on optimum deposition conditions, new types of alloys, and dedicated interface passivation layers. In terms of industrialization, the competition is fierce for standard PV applications and there is a clear need for higher efficiency or to secure captive markets for the current producers of thin-film silicon PV modules. Even though the market for BIPV application has not grown as expected, thin-film silicon is still of particular interest to this sector, as demonstrated in Fig. 6. Indeed, it offers a proven degree of flexibility in transparency, color, size and substrate type, together with the necessary durability and environmental friendliness, at a price potentially as low as that of conventional tiles. At a time where zero-energy building should become the norm, it is worth considering engaging such markets more actively.

Finally, we should mention that many of the developments presented here can be of interest for other fields. For instance, high-quality silicon material can be used in high-efficiency c-Si heterojunction cells, where a very thin layer of a-Si:H is used as passivating layer on c-Si wafers [117]. a-Si:H has also been used in a novel generation of 'micro-channel plate' detectors [118], while μc-Si:H can be of interest for higher mobility thin-film transistors, and can be manufactured in existing plasma reactors for application in displays (see, e.g. [119]).

Acknowledgements

The authors gratefully acknowledge support by the Swiss Federal Office of Energy under project no SI/500750-01 as well as the Swiss Competence Center for Energy and Mobility (CCEM-CH) and Swisselectric Research (in the framework of the project 'DURSOL'). Part of the work reported here was also carried out in the framework of the FP7 projects 'Fast Track' and 'PEPPER', funded by the EC under grant agreements nos. 283501 and 249782, respectively. Finally, the authors thank Mustapha Benkhaira and Pasqualina Pettoruto for the deposition of LPCVD ZnO electrodes, as well as Massoud Dadras and Mireille Leboeuf for the preparation of samples and TEM measurements.

References

[1] A. Jäger-Waldau, PV Status Report, Scientific and Policy Report by the Joint Research Center of the European Commission, 2013.
[2] A. Feltrin, A. Freundlich, Renew. Energy 33 (2) (2008) 180.
[3] J. Yang, A. Banerjee, S. Guha, Sol. Energy Mater. Sol. Cells 78 (2003) 597.
[4] C.-Y. Tsai, C.-Y. Tsai, J. Nanomater. (2014), http://dx.doi.org/10.1155/2014/809261.
[5] P. Heinstein, C. Ballif, L.-E. Perret-Aebi, Green 3 (2014) 125.
[6] D.L. Staebler, C.R. Wronski, Appl. Phys. Lett. 31 (1977) 292.
[7] A. Shah (Ed.), Thin-Film Silicon Solar Cells, CRC Press, 2010.
[8] M. Izu, T. Ellison, Sol. Energy Mater. Sol. Cells 78 (2003) 613.
[9] S. Guha, J. Yang, B. Yan, in: B. Pallab, F. Roberto, K. Hiroshi (Eds.), Comprehensive Semiconductor Science and Technology, Elsevier, Amsterdam, The Netherlands, 2011, pp. 308–352.
[10] A. Bernasconi, et al. Proc. of the 4th World Conference on PV Energy Conversion, 2006, . p. 2312.
[11] J. Meier, et al. Proc. of the 24th IEEE PVSC, 1994, . p. 409.
[12] P. Cuony, et al. Adv. Mater. 24 (2012) 1182.
[13] K. Yamamoto, et al. Solar Energy 77 (2004) 939.
[14] A. Lambertz, et al. Proc. of the 22th European Photovoltaic Solar Energy Conference, 2007, . p. 1839.
[15] P. Buehlmann, et al. Appl. Phys. Lett. 91 (2007) 143505.
[16] M. Boccard, et al. Solar Energy Mater. Sol. Cells 119 (2013) 12.
[17] B. Niesen, et al. Nano Lett. 14 (9) (2014) 5085.
[18] R. Biron, et al. Solar Energy Mater. Sol. Cells 114 (2013) 147.
[19] M. Stuckelberger, et al. Prog. Photovolt.: Res. Appl. (2014), http://dx.doi.org/10.1002/pip.2559.
[20] H. Cotal, et al. Energy Environ. Sci. 2 (2009) 174.
[21] A. De Vos, J. Phys. D: Appl. Phys. 13 (1980) 839.
[22] F. Meillaud, et al. Sol. Energy Mater. Sol. Cells 90 (18–19) (2006) 2952.
[23] S. Benagli, et al. Proc. of the 24th European Photovoltaic Solar Energy Conference, 2009, . p. 2293.
[24] M.A. Green, et al. Prog. Photovolt: Res. Appl. 22 (2014) 701.
[25] C. Ballif, et al. 29th European Photovoltaic Solar Energy Conference, 2014, 3CP1.1.
[26] M. Boccard, et al. IEEE J. Photovolt. 4 (6) (2014) 1368.
[27] D.J. You, et al. Prog. Photovolt: Res. Appl. (2014), http://dx.doi.org/10.1002/pip.2510.
[28] TEL Press Release, 2014, July 9, http://www.solar.tel.com.
[29] B. Stannowski, et al. Solar Energy Mater. Sol. Cells 119 (2013) 196.
[30] S. Smith, M.J. Shaio, Solar PV Balance of System (BOS) Markets: Technologies, Costs and Leading Companies, 2013–2016, Greentech Media Inc., 2012.
[31] H. Sai, et al. 75th JSAP Autumn Meeting, 2014.
[32] S. Guha, J. Yang, B. Yan, Solar Energy Mater. Sol. Cells 119 (2013) 1.
[33] M.A. Green, et al. Prog. Photovolt.: Res. Appl. 21 (2013) 1.
[34] B. Yan, et al. Appl. Phys. Lett. 99 (11) (2011) 113512.
[35] O. Isabella, A. Smets, M. Zeman, Solar Energy Mater. Sol. Cells 129 (2014) 82.
[36] J. Haschke, et al. SOLMAT 128 (2014) 190–197.
[37] J. Dore, et al. IEEE JPV 4 (1) (2014) 33.
[38] D. Amkreutz, et al. IEEE JPV 4 (6) (2014) 1496.
[39] A.A. Howling, et al. Natl. Symp. Am. Vac. Soc. 10 (4) (1992) 1080.
[40] W. Schwarzenbach, J. Vac. Sci. Technol. A: Vac. Surf. Films 14 (1) (1996) 132.
[41] E. Amanatides, D. Mataras, D.E. Rapakoulias, J. Vac. Sci. Technol. A: Vac. Surf. Films 20 (1) (2002) 68.
[42] B. Rech, et al. Thin Solid Films 427 (2003) 157.
[43] Y. Takeuchi, et al. Jap. J. Appl. Phys. 40 (Pt 1 (5A)) (2001) 3405.
[44] C. Niikura, M. Kondo, A. Matsuda, J. Non-Cryst. Solids 338–340 (2004) 42.
[45] O. Vetterl, et al. Sol. Energy Mater. Sol. Cells 62 (1–2) (2000) 97.
[46] B. Strahm, et al. Sol. Energy Mater. Sol. Cells 91 (6) (2007) 495.
[47] H. Sakai, et al. Jap. J. Appl. Phys. 29 (Pt 1 (4)) (1990) 630–635.
[48] E. Vallat-Sauvain, et al. J. Non-Cryst. Solids 352 (2006) 1200.
[49] F. Meillaud, et al. Proc. of the 31st IEEE Photovoltaic Specialists Conference, 2005, . p. 1412.
[50] S. Kasouit, et al. J. Non-Cryst. Solids 299–302 (2002) 113.
[51] A.H.M. Smets, T. Matsui, M. Kondo, J. Appl. Phys. 104 (2008) 034508.
[52] U. Kroll, et al. Solar Energy Mater. Sol. Cells 48 (1997) 343.
[53] L. Guo, et al. Jap. J. Appl. Phys. 37 (1998) 1116.
[54] M. Kondo, Solar Energy Mater. Sol. Cells 78 (2003) 543.
[55] T. Matsui, A. Matsuda, M. Kondo, Solar. Energy Mater. Solar Cells 90 (2006) 3199.
[56] Y. Nakano, et al. Thin Solid Films 506–507 (2006) 33.
[57] M. Matsumoto, et al. IEEE J. Photovolt. 3 (1) (2013) 35.
[58] P. Roca i Cabarrocas, et al. Appl. Phys. Lett. 66 (1995) 3609.
[59] K. Mori, et al. Jap. J. Appl. Phys. 39 (2000) 6647.
[60] J. Bailat, et al. J. Non-Cryst. Solids 299–302 (2002) 1219.
[61] H. Yamamoto, et al. Proc. of the 11th European Photovoltaic Solar Energy Conference, 1999, . p. 231.
[62] Y. Nasuno, M. Kondo, A. Matsuda, Jap. J. Appl. Phys. 40 (2001) L303.
[63] M. Python, et al. J. Non-Cryst. Solids 354 (19–25) (2008) 2258.
[64] S. Hänni, et al. IEEE J. Photovolt. 3 (1) (2013) 11.
[65] S. Nicolay, S. Faÿ, C. Ballif, Cryst. Growth Design 9 (2009) 4957.
[66] J. Bailat, et al. Proc of the 4th World Conference on Photovoltaic Solar Energy Conversion, 2006, . p. 1533.
[67] M. Python, et al. Prog. Photovolt.: Res. Appl. 18 (2010) 491.
[68] G. Bugnon, et al. Adv. Funct. Mater. 22 (17) (2012) 3665.
[69] G. Bugnon, High-Quality Microcrystalline Silicon for Efficient Thin-Film Solar Cells: Insights into Plasma and Material Properties, PhD thesis, EPFL, 2013.
[70] A. Matsuda, et al. Jap. J. Appl. Phys. 43 (12) (2004) 7909.
[71] D. Chaudhary, et al. Proc. of the 27th European Photovoltaic Solar Energy Conference, 2012, . p. 2094.
[72] S. Hänni, et al. Proc. of the 26th European Photovoltaic Solar Energy Conference, 2011, . p. 2699.
[73] S.R. Ovshinsky, A. Madan, Nature 276 (1978) 483.
[74] S. Kasouit, J. Non-Cryst. Solids 338–340 (2004) 369.
[75] S. Hänni, Microcrystalline Silicon for High-Efficiency Thin-Film Photovoltaic Devices, PhD thesis, EPFL, 2014.
[76] Q. Zhang, et al. Phys. Status Solidi A: Rapid Res. Lett. 2 (4) (2008) 154.
[77] J.-C. Dornstetter, S. Kasouit, P. Roca i Cabarrocas, IEEE J. Photovolt. 3 (1) (2013) 581.
[78] M. Moreno, R. Boubekri, P. Roca i Cabarrocas, Solar Energy Mater. Sol. Cells 100 (2012) 16.
[79] J. Meier, et al. Solar Energy 77 (2004) 983.
[80] S. Shimizu, M. Kondo, A. Matsuda, J. Appl. Phys. 97 (2005) 033522.
[81] J. Koh, et al. Appl. Phys. Lett. 73 (1998) 1526.
[82] P. Roca i Cabarrocas, et al. Thin Solid Films 403–404 (2002) 39.
[83] M. Stuckelberger, et al. J. Appl. Phys. 114 (2013) 154509.
[84] T. Matsui, et al. Prog. Photovolt.: Res. Appl. 21 (2013) 1363.
[85] S. Chattopadhyay, et al. Mater. Sci. Eng. Rep. 69 (2010) 1.
[86] J. Escarré, et al. Solar Energy Mater. Sol. Cells 98 (2012) 185–190.
[87] T. Matsui, et al. Proc. of the 20th European Photovoltaic Solar Energy Conference, 2005, . p. 1493.
[88] M. Kambe, et al. Tech. Digest of the 17th International Photovoltaic Science and Engineering Conference, 2007, . p. 1161.
[89] J. Bailat, et al. Proc. of the 25th European Photovoltaic Solar Energy Conference, 2010, . p. 2720.
[90] J. Escarré, et al. Solar Energy Mater. Sol. Cells 95 (2011) 881.
[91] C. Battaglia, et al. Nat. Photonics 5 (2011) 535.
[92] M. Boccard, et al. IEEE J. Photovolt. 2 (2012) 83.
[93] H. Sai, K. Saito, M. Kondo:, Appl. Phys. Lett. 101 (2012) 173901.
[94] H. Sai, et al. Appl. Phys. Lett. 98 (2011) 113502.
[95] K. Söderström, J. Appl. Phys. 112 (2012) 114503.
[96] S. Misra, et al. J. Phys. D: Appl. Phys. 47 (2014) 393001.
[97] H.W. Deckman, et al. Appl. Phys. Lett. 42 (1983) 110968.
[98] M. Boccard, et al. Appl. Phys. Lett. 101 (2012) 151105.
[99] M. Berginski, et al. J. Appl. Phys. 101 (2007) 074903.
[100] M. Boccard, et al. EPJ Photovolt. 5 (2014) 50601.
[101] F. Ruske, et al. J. Appl. Phys. 107 (1) (2010) 013708.
[102] L. Ding, et al. Solar Energy Mater. Sol. Cells 98 (2012) 331.
[103] T. Koida, H. Fujiwara, M. Kondo, Jap. J. Appl. Phys. 46 (2007) L685.
[104] C. Battaglia, et al. J. Appl. Phys. 109 (2011) 114501.
[105] J. Krc, et al. Appl. Phys. Lett. 94 (2009) 153501.
[106] O. Isabella, et al. MRS Proc. 1153 (2009) 41.
[107] P. Sichanugrist, et al. J. Non-Cryst. Solids 164–166 (2) (1993) 1081.
[108] P. Cuony, et al. Appl. Phys. Lett. 97 (21) (2010) 213502.
[109] F. Finger, et al. Thin Solid Films 517 (12) (2009) 3507–3512.
[110] T. Chen, et al. Sol. Energy Mater. Sol. Cells 98 (2012) 370.
[111] M. Despeisse, et al. Appl. Phys. Lett. 96 (2010) 073507.
[112] G. Bugnon, et al. Solar Energy Mater. Sol. Cells 120 (2014) 143.
[113] H. Sakai, et al. J. Appl. Phys. 67 (1990) 3494.
[114] T. Söderström, et al. J. Appl. Phys. 104 (2008) 104505.
[115] G. Yue, et al. J. Non-Cryst. Solids 354 (2008) 2440.
[116] S. Hänni, et al. Phys. Status Solidi A 1–6 (2015), http://dx.doi.org/10.1002/pssa.201431708.
[117] S. De Wolf, et al. Green 2 (1) (2012) 7.
[118] A. Franco, et al. Sci. Rep. 4 (2014) 4597.
[119] C.-H. Lee, et al. Appl. Phys. Lett. 89 (2006) 252101.